Phosphorylation of the Growth Arrest-specific Protein Gas2 Is Coupled to Actin Rearrangements during Go→G1 Transition in NIH 3T3 Cells

Claudio Brancolini,* and Claudio Schneider*‡

Laboratorio Nazionale Consorzio Interuniversitario, Biotecnologie, AREA Science Park, 34142 Trieste, Italy; and ‡Dipartimento di Scienze e Technologie Biomediche, Sezione di Biologia, Universitá di Udine, 33100 Udine, Italy

Abstract. Growth arrest-specific (Gas2) protein has been shown to be a component of the microfilament system, that is highly expressed in growth arrested mouse and human fibroblasts and is hyperphosphorylated upon serum stimulation of quiescent cells. (Brancolini, C., S. Bottega, and C. Schneider. 1992. *J. Cell Biol.* 117:1251-1261). In this study we demonstrate that the kinetics of Gas2 phosphorylation, during Go→G1 transition, as induced by addition of 20% FCS to serum starved NIH 3T3 cells, is temporally coupled to the reorganization of actin cytoskeleton.

To better dissect the relationship between Gas2 phosphorylation and the modification of the microfilament architecture we used specific stimuli for both membrane ruffling (PDGF and PMA) and stress fiber formation (L-α-lysophosphatidic acid LPA) (Ridley, A. J., and A. Hall. 1992. *Cell.* 70:389-399). All of them, similarly to 20% FCS, are able to downregulate Gas2 biosynthesis. PDGF and PMA induce Gas2 hyperphosphorylation that is temporally coupled with the appearance of membrane ruffling where Gas2 localizes. On the other hand LPA, a specific stimulus for stress fiber formation, fails to induce a detectable Gas2 hyperphosphorylation.

Thus, Gas2 hyperphosphorylation is specifically correlated with the formation of membrane ruffling possibly implying a role of Gas2 in this process.

When growth factors are removed from nutrient-containing medium, cultured fibroblasts leave the cell cycle and enter a quiescent state. Cell cycle reentry requires addition of serum or growth factors to quiescent cells: the complex response that is elicited is called Go→G1 transition (1).

Binding of growth factors to tyrosine kinase receptors, at the cell surface, is followed by receptor dimerization which seems to be responsible for the activation of the protein tyrosine kinase activity and autophosphorylation of the receptor cytoplasmic domain (53). The tyrosine autophosphorylated regions of growth factor receptors act as binding sites for signalling molecules containing the *src* homology 2 (SH2)[1] domain (30).

Tyrosine phosphorylation of target signaling proteins is followed by activation of several serine/threonine protein kinases such as *raf*, MAP, PKC, and the S6 kinase family (16, 29, 32, 51). These represent a "second wave" of phosphorylation, which amplifies the initial tyrosine phosphorylation-dependent message. As a result of this phosphorylation cascade, depending on the type of tyrosine kinase receptor and its cellular context (signalling molecules), cells respond with the induction of DNA synthesis (8). Signal transduction through growth factor receptors leads to a well-defined nuclear response by inducing the expression of immediate early response genes (27), among which proto-oncogenes such as c-*fos* and c-*myc* have been identified (11, 21). These represent positive circuit elements that are necessary for cell cycle progression, since their ablation by antisense RNA or by specific antibodies prevents DNA synthesis in different cellular systems (24, 31).

Another facet of the Go→G1 transition as determined by the presence of serum and growth factors is the downregulation of the expression of a set of *gas* (growth arrest specific) genes (45) that are highly expressed under quiescence. These genes may represent negative circuit elements that must be downregulated to allow cell cycle progression (46). Indeed, this hypothesis has proven correct in the case of *gas*1 gene, whose forced expression during the Go→G1 transition does not allow entry into S phase (14).

The biochemical and genetic alterations induced by serum/

Address all correspondence to C. Brancolini, LNCIB, Area Science Park, Padriciano 99, 34012 Trieste, Italy.

1. *Abbreviations used in this paper*: BrdUrd, bromodeoxyuridine; CMR, circular membrane ruffling; DCS, donor calf serum; Gas, growth arrest specific; GST, glutathionine-s-transferase; LPA, L-α-lysophosphatidic acid; MARCKS, myristoylated alanine-rich C kinase substrata; SH2, src homology 2.

growth factors addition to quiescent cells are generally coupled with morphological changes (9). Cell shape is maintained by a complex network of factors including cytoskeletal components, cytoskeleton associated elements, and membrane–cytoskeleton coupling factors (49). The microfilament network system is the most characterized component of the cytoskeleton described to undergo well-defined rearrangements during the Go→G1 transition (3, 26). Some microfilament-associated proteins have been shown to be phosphorylated either in tyr or ser/thr after growth factor stimulation (6). Furthermore the actin-binding protein tensin, has been shown to contain SH2 domains (13) thus relating to the signal transduction machinery via phosphorylation to specific target/transducer for actin remodelling. The tight relation between second messenger generation and actin rearrangement has been firmly established for profilin (for review see references 2, 19). However, it is still an open question whether the microfilament network plays a direct role in the generation of growth-regulating signals or is only required to generate motility and chemotactic responses, that are coupled but independent events in the growth cycle program.

The identification and characterization of new components of the microfilament system, whose expression is tightly linked to the growth state (7, 18, 54) may represent an important step to elucidate the involvement of the microfilament system in growth control. A good candidate for this class of proteins is Gas2 that we have previously shown to be a component of the microfilament system, whose expression is highly induced under growth arrest both in mouse and human fibroblasts (5).

In this work we analyze the relationship between the kinetics of Gas2 phosphorylation and the specific modifications of actin cytoskeleton in serum-starved cells triggered by addition of the following mitogenic stimuli: 20% FCS, PDGF, L-α-lysophosphatidic acid (LPA), and PMA. Each of these stimuli is able to induce down-regulation of Gas2 biosynthesis. Gas2 hyperphosphorylation is specifically induced by 20% FCS, PDGF, and PMA and its kinetics is temporally coupled to the formation of membrane ruffling, where Gas2 localizes. On the other hand LPA, which is a specific inducer of stress fibers (38) fails to stimulate a significant level of Gas2 hyperphosphorylation.

Materials and Methods

Cell Lines and Culture Conditions

NIH 3T3 were routinely cultured in DME with 10% FCS. In each experiment 5×10^4 cells/ml were seeded in a 35 mm Petri dishes.

For serum starvation, medium was changed to 0.5% FCS when cells were subconfluent; cells were then left in this medium for 48 h. After incubation with 50 μM bromodeoxyuridine (BrdUrd) for an additional 1 h less than 3% of the nuclei were labeled. For induction of DNA synthesis, fresh medium containing 20% FCS was added to the arrested cells. After 18 h from addition of serum and a 1-h pulse with BrdUrd, ~90% of the nuclei resulted positive for BrdUrd incorporation.

PDGF (kindly provided by Dr. B. Westermak, University of Uppsala, Uppsala, Sweden) was used at a final concentration of 40 ng/ml; LPA (Sigma Immunochemicals, St. Louis, MO) was used at a final concentration of 70 μM in medium containing 0.5% FCS.

NIH 3T3 mouse fibroblasts type A (a gift of Dr. M. Crescenzi University of Rome, Rome, Italy) were used for all the PMA experiments. These cells were cultured in DME with 10% donor calf serum (DCS). Serum-starved NIH 3T3A were induced into the growing cycle by addition of fresh medium containing 20% FCS. Under these conditions ~90% of the cells were in S phase, as analyzed by BrdUrd incorporation, after 15 h from FCS addition. DNA synthesis assays were performed as previously described (5).

Cell Labeling and Immunoprecipitation

For ^{32}P labeling, NIH 3T3 cells were cultured in 35 mm petri dishes for 43 h in 0.5% FCS; after this time phosphate-free medium containing 0.2 mCi/ml ^{32}Pi and 0.5% FCS was added and left for further 5 h. At the end of the labeling period, cells were either stimulated for the indicated times by addition of 20% FCS, PMA (10^{-7} M), PDGF (40 ng/ml), LPA (70 μM), or left in the same labeling medium (resting cells).

For methionine labeling, serum-starved and mitogen-treated cells, were labeled for 3 h in 1 ml of DME methionine-free, containing 400 μCi/ml [^{35}S]methionine (ICN, Irvine, CA; Trans^{35}S label 1,133 Ci/mmole 492 TBq/mmole).

After washing with cold PBS, cells were lysed on the dish by addition of 0.5 ml lysis buffer (150 mM NaCl, 20 mM TEA, pH 7.5, 0.1% NP-40). After 1 min on ice the detergent-soluble supernatant was removed and made 0.8% SDS final concentration before boiling for 4 min 0.5 ml of quench buffer (100 mM NaCl, 20 mM TEA, pH 7.5, 4% Triton X-100) was then added containing (final concentrations) 1 mM PMSF and 10 μg/ml each of aprotinin, leupeptin, antipain, and pepstatin. The lysates were cleared by centrifugation in an Eppendorf centrifuge (Brinkman Instruments Inc., Westbury, NY) for 2 min. The supernatants were incubated with 30 μl of normal rabbit serum for 1 h at 4°C and transferred to a new Eppendorf tube containing 20-μl wet volume pellet of prewashed Staph A. After resuspension of the Staph A, the lysates were incubated by continuous rocking at 4°C, for 30 min, and then centrifuged for 2 min in Eppendorf centrifuge. This was repeated once more and the lysates were finally centrifuged for 10 min in an Eppendorf centrifuge. The resulting supernatants were then used for immunoprecipitation by incubation with the affinity-purified anti-Gas2 antibody (5) for 3 h at 4°C with rocking. Finally, 80 μl of protein A–Sepharose (10% wt/vol) suspension was added and the incubation was continued for 1/2 h by rocking at 4°C. Protein A–Sepharose was recovered by centrifugation, washed three times in wash buffer (20 mM TEA, pH 7.5, 150 mM NaCl, 0.5% Triton-X 100, 1 mM PMSF), and then finally resuspended in SDS-PAGE sample buffer. Immune complexes were released by boiling for 5 min.

For phosphoamino acid analysis lysis buffer was supplemented with 0.1 mM $NaVO_4$.

In Vitro Kinase Assay

NIH 3T3 cells were grown in plastic tissue culture dishes (15-cm diam). Serum-deprived or -activated cells, at different time points, were washed twice with 10 ml of ice cold phosphate-buffered saline, scraped using a rubber policeman, and sedimented by centrifugation at 1,000 rpm for 5 min at 4°C (in a Braun centrifuge 3K12; Braun Biotech International, Melsungen, Germany). The pellets were resuspended in 200 μl of kinase/lysis buffer containing: 150 mM NaCl, 0.1% NP-40, 2 mM PMSF, 20 mM TEA, pH 7.5, 20 mM $MgCl_2$, 2 μM $MnCl_2$, 5 mM *p*-nitrophenylphosphate, 100 nM Microcystine-LR, and 10 nM Okadaic acid. The nuclear pellet was discarded after centrifugation for 5 min at 800 *g* in a centrifuge (J2-21M/E; Beckman Instruments, Palo Alto, CA). The supernatants were centrifugated for 15 min at 20,000 *g* in a centrifuge (J2-21M/E; Beckman Instruments) at 4°C.

10-μl aliquots were analyzed by SDS-PAGE gels to standardize the amount of the protein contained in the cellular extracts derived from the different time points. The cellular lysates were frozen at −80°C and used within 24 h for the in vitro kinase assay. The in vitro kinase assay was performed using 80 μl of cellular lysates and ~3 μg each of glutathione-s-transferase (GST)–Gas2 fusion protein or GST (5), 20 μM rATP, and 10–30 μCi of γ-^{32}-labeled PATP (Amersham Corp., Arlington Heights, IL; 3,000 Ci/mmole, 110 TBq/mmole) for 30 min at 30°C. The GST or GST-Gas2 fusion protein were purified by incubation of cellular lysates with glutathione–Sepharose beads at 4°C for 30 min. After six washes in washing buffer (4 M urea, 1% Triton X-100, 20 mM TEA, pH 7.5, 150 mM NaCl) the samples were released by boiling for 3 min in SDS-PAGE sample buffer. The supernatants were then analyzed by SDS-PAGE followed by Coomassie staining and autoradiography.

Phosphoamino Acid Analysis

The phosphoamino acid composition was analyzed as previously described

(44). Polyacrilamide gels (15%) containing the immunoprecipitated Gas2 protein labeled in vivo with ^{32}Pi or the GST-Gas2 fusion protein labeled in vitro, were blotted (4) onto Immobilon PVDF membrane (Milligene; Millipore Corp., Bedford, MA). Bands containing ^{32}P-labeled proteins were located by autoradiography, excised, and subjected to direct hydrolysis in 5.7 M HCl at 110°C for 75 min as described (28).

High-voltage TLC electrophoresis was performed at 2,000 V for 15 min used pyridine/glacial acetic acid/H_2O (5:50:945 ml) buffer system.

Subcellular Fractionation

For subcellular fractionation analysis, serum-starved NIH 3T3 cells were labeled for 12 h with 200 μCi [^{35}S]methionine; 20% FCS was then added for the indicated times as described. To obtain the detergent-soluble and -insoluble fractions cell monolayers were incubated with 0.5 ml Triton X-100 lysis buffer (300 mM sucrose, 0.2% Triton X-100, 100 mM NaCl, 1 mM EGTA, 3 mM $MgCl_2$, 10 mM Pipes, pH 6.9, 1 mM PMSF) for 40 s on ice. Solubilized material was collected as the detergent-soluble fraction. The material remaining on the petri dish was scraped using a rubber policeman in 0.5 ml of the lysis buffer containing 0.8% SDS (detergent-insoluble preparation). Immunoprecipitations were performed as described above.

To obtain the membrane or cytoplasmic fractions hypotonic cell lysis was used followed by differential centrifugation (12). NIH 3T3 cells, labeled with [^{35}S]methioine after 48 h of serum starvation, were treated with 20% FCS for the indicated times, rinsed twice with cold PBS, and scraped into 0.5 ml of cold PBS. The cells were centrifuged at 1,000 *g* for 5 min at 4°C, resuspended in 0.5 ml of swelling buffer (5 mM KCl, 15 mM Tris, pH 7.5, 1 mM PMSF, and 10 μg/ml each of aprotinin, leupeptin, antipain, and pepstatin) and incubated for 20 min on ice, and then subjected to 25 strokes in a glass Dounce homogenizer type B (Kontes Glass Co., Vineland, NJ). Crude membrane fraction was prepared by centrifugation at 100,000 *g* for 60 min at 4°C (Beckman ultracentrifuge OPTIMAL-TL). The resulting pellet, was resuspended in 0.5 ml of lysis buffer (150 mM NaCl, 20 mM TEA, pH 7.5, 0.8% SDS, and 1 mM PMSF) and processed for immunoprecipitation as described above. The supernatant was used as such for the subsequent immunoprecipitation.

Immunofluorescence Microscopy

For indirect immunofluorescence microscopy, cultured NIH 3T3 cells were grown under the described conditions, and then fixed with 3% paraformaldehyde in PBS for 20 min at room temperature. Fixed cells were washed with PBS/0.1 M glycine, pH 7.5, and then permeabilized with 0.1% Triton X-100 in PBS for 5 min. The coverslips were treated with the first antibody (anti-Gas2 diluted in PBS 3% BSA) for 1 h in a moist chamber at 37°C. They were then washed with PBS three times, followed by incubation with biotinylated anti-rabbit second antibody (Southern Biotechnology Associates, Birmingham, AL) for 1 h at 37°C. The immunocomplexes were visualized by incubation with streptavidin rhodamine conjugated (Jackson ImmunoResearch Labs., Inc., West Grove, PA). For detection of actin filaments, FITC-phalloidin (Sigma Inmunochemicals) was used. In the case of simultaneous detection of Gas2 and transferrin receptor, after fixation and washing with PBS/0.1 M glycine, pH 7.5, the coverslips were directly treated with the monoclonal antibody against the transferrin receptor (rat anti-CD 71; Pharmingen, San Diego, CA) to visualize only the cell surface exposed receptor. After three washes with PBS coverslips were incubated with anti-rat fluoresceine-conjugated second antibody (Southern Biotechnology Associates). After extensive washes cells were permeabilized with 0.1% Triton X-100 in PBS to perform Gas2 immunolocalization as described above. Cells were examined by epifluorescence with a Zeiss Axiovert 35 microscope or a Zeiss laser scan microscope (LSM 410) equipped with a 488 λ argon laser and a 543 λ helium neon laser. The following set of filters were used: rhodamine (BP546, FT580, LP 590); fluoresceine (450-490, FT 510, LP520).

Results

In Vivo Analysis of Gas2 Phosphorylation

The results of previous work from this laboratory (5, 45) indicated two distinct levels of regulation of Gas2 protein during the Go→G1 transition. First, *gas2* mRNA expression decreases during the first hours from addition of serum to quiescent cells with a consequent downregulation of Gas2 biosynthesis (5, 45). A second level of regulation is suggested by the observation that Gas2 protein becomes efficiently hyperphosphorylated after serum stimulation (5).

We thus decided to analyze in closer detail the kinetics of in vivo Gas2 phosphorylation after serum addition.

Serum-starved NIH 3T3 cells were labeled with ^{32}P and treated with 20% FCS for the indicated times. Equal numbers of TCA-precipitable counts from cellular lysates were then immunoprecipitated with anti-Gas2 antibodies.

Fig. 1 *a* shows that addition of serum to quiescent cells induces an increased phosphorylation of Gas2, which is clearly detectable after 5 min from serum stimulation. This level of phosphorylation is maintained up to 3 h from the addition of 20% FCS (Fig. 1 *b*).

The phosphoamino acids present in Gas2 protein immunoprecipitated from lysates of cells activated with serum for 30 min were analyzed and shown to be phospho-serine (Fig. 1 *c*).

In Vitro Analysis of Gas2 Phosphorylation

To more precisely map the kinetics of activation of the Gas2-specific kinase we developed an in vitro assay based on the purified GST-Gas2 fusion protein produced in *Escherichia coli* (5) as a substrate for the kinase. Cellular extracts were prepared from serum-starved cells and after different times

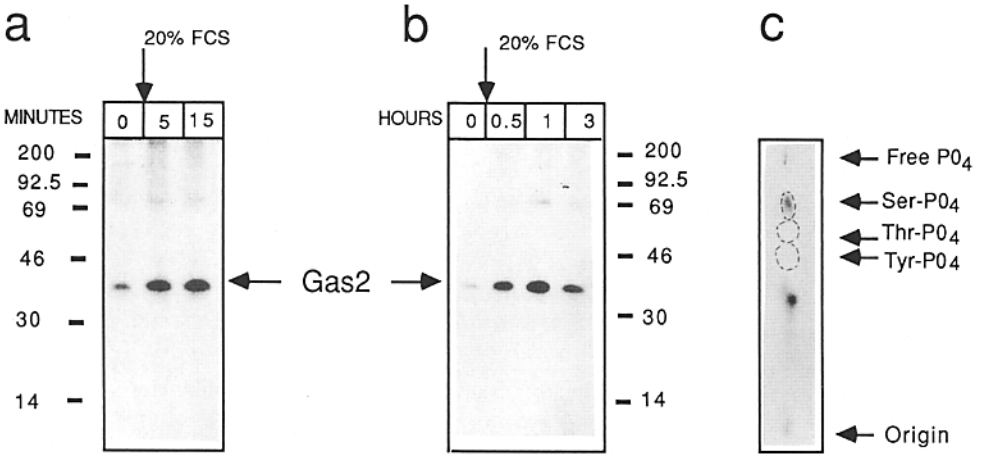

Figure 1. In vivo phosphorylation analysis of Gas2 after addition of 20% FCS to serum-starved NIH 3T3 cells. (*a* and *b*) Serum-starved NIH 3T3 cells (*0*) or serum activated for the indicated times were prelabeled for 5 h with ^{32}Pi. After cell lysis immunoprecipitations were performed using the same number of cpm. (*c*) Phosphoaminoacid analysis of in vivo phosphorylated Gas2 30 min after 20% FCS addition to serum-starved cells.

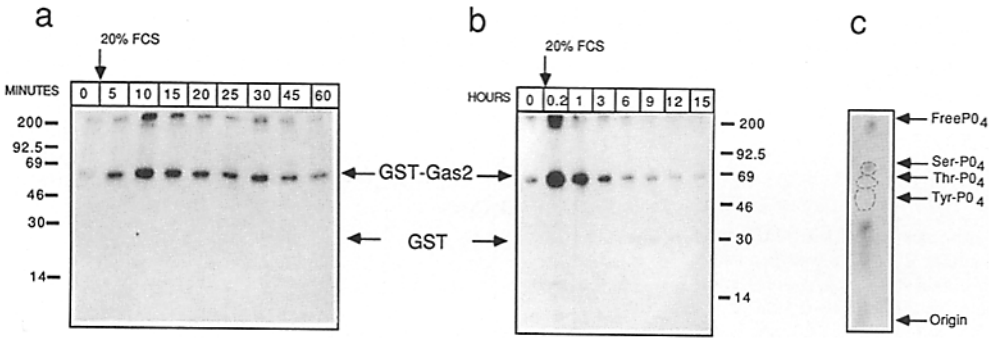

Figure 2. In vitro phosphorylation of GST-Gas2 fusion protein. (*a* and *b*) Cellular extracts from serum-starved NIH 3T3 cells (*0*) or at the indicated times after 20% FCS addition were used to perform in vitro phosphorylation as described in material and methods. (*c*) Phosphoaminoacid analysis of in vitro phosphorylated GST-Gas2 fusion protein using cellular extracts prepared from NIH 3T3 cells stimulated for 10 min with 20% FCS.

from serum stimulation. These lysates were incubated with a GST-Gas2 fusion protein in the presence of ^{32}P-labeled γ-ATP. The GST-Gas2 and GST control proteins were recovered using glutathione-Sepharose beads, eluted from the beads by boiling in SDS sample buffer and analyzed by SDS-PAGE.

Fig. 2 *a* shows the results of such an analysis performed during the Go→G1 transition. One prominent band, corresponding in size to the GST-Gas2 fusion protein, is the only detectable phosphorylation product while GST control substrate (see *arrow*, corresponding to the Coomassie blue-stained GST protein) is undetectable. Both GST-Gas2 fusion protein and GST control were used at the same relative levels as confirmed by Coomassie blue staining of the same gel. From this we can confirm that the phosphorylation target present in the chimera GST-Gas2 can be ascribed to the Gas2 protein component.

The timing of appearance of the kinase activity in this in vitro assay should thus reflect the in vivo kinetics of Gas2 phosphorylation. In fact, kinase activity is present at a low level in quiescent cells and becomes detectable after 5 min from serum stimulation, reaching its maximum at 10 min, and remaining at a comparable level 30 min from the activation. After this time it decreases as evidenced when the analysis is performed in an expanded time scale as shown in Fig. 2 *b*, where a peak in kinase activity is reached after 10 min from serum stimulation, but it clearly decreases after 1 h from serum stimulation. A basal level of activity is reached at 6 h from serum addition; ^{32}P incorporation remains constantly undetectable in the GST control substrate (see *arrow*, Fig. 2 *b*).

When the phosphoaminoacid analysis is performed on the GST-Gas2 fusion protein incubated with an extract of cells treated with 20% FCS for 10 min; we find that Gas2 is also phosphorylated on serine residues (Fig. 2 *c*).

Gas2 Localization in Quiescent and Serum-activated NIH 3T3 Cells as detected by Biochemical Fractionation

We have previously shown that Gas2 is a component of the microfilament network system which can be extracted following treatment of growth arrested cells with nonionic detergents (5). We decided to use mild detergent extraction conditions which preserve weak interactions (22), to better define Gas2 distribution between detergent soluble/insoluble fractions during Go→G1 transition as induced by serum.

Serum-starved cells were labeled with [^{35}S]methionine in 0.5% FCS and 20% FCS was then added for the indicated times. Detergent-soluble and -insoluble fractions were prepared, as described in material and methods, from each time point, and immunoprecipitations were performed using equal numbers of TCA-precipitable counts.

Fig. 3 *a* shows that Gas2 is almost equally distributed between detergent-soluble and -insoluble fractions and this pattern does not seem to change upon serum stimulation. Similar results were obtained when cells were labeled with ^{32}P (data not shown).

Next, we decided to analyze whether Gas2 can interact with cellular membranes. NIH 3T3 cells labeled with [^{35}S]-methionine under serum starvation were used as such or stimulated with 20% FCS. After differential centrifugation (see Material and Methods), the resulting membrane (pellet) and cytosol (SN) fractions were subjected to immunoprecipitation analysis using Gas2 antibody. Gas2 is detectable in the crude membrane fraction both in serum-starved and -activated cells (Fig. 3 *b*). The marked asterisk points to the precipitation of a non-specific product that seems to be exclusively present in the soluble cytoplasmic fractions, thus indicating the degree of fractionation. The quality of the fractionation was also confirmed by performing immunoprecipitation with transferrin receptor antibody, an integral membrane protein marker (44) and affinity chromatography of the cellular glutathione-S-transferase (47), as a marker for soluble proteins. The lower panels show such an analysis. As expected, the transferrin receptor is exclusively present in the membrane fractions, while endogenous GST is predominantly present in the cytosolic fraction. The low amount of GST detectable in the membrane fraction could be either due to specific or non-specific interaction with cellular membranes. These data strengthen the idea that Gas2 can interact either directly or indirectly with cellular membranes.

Gas2 Localization in Quiescent and Serum-stimulated NIH 3T3 Cells as Detected by Immunofluorescence Analysis

As already described (38, 39) the microfilament system undergoes two most easily detectable changes after serum stimulation of quiescent fibroblasts: membrane ruffling and stress

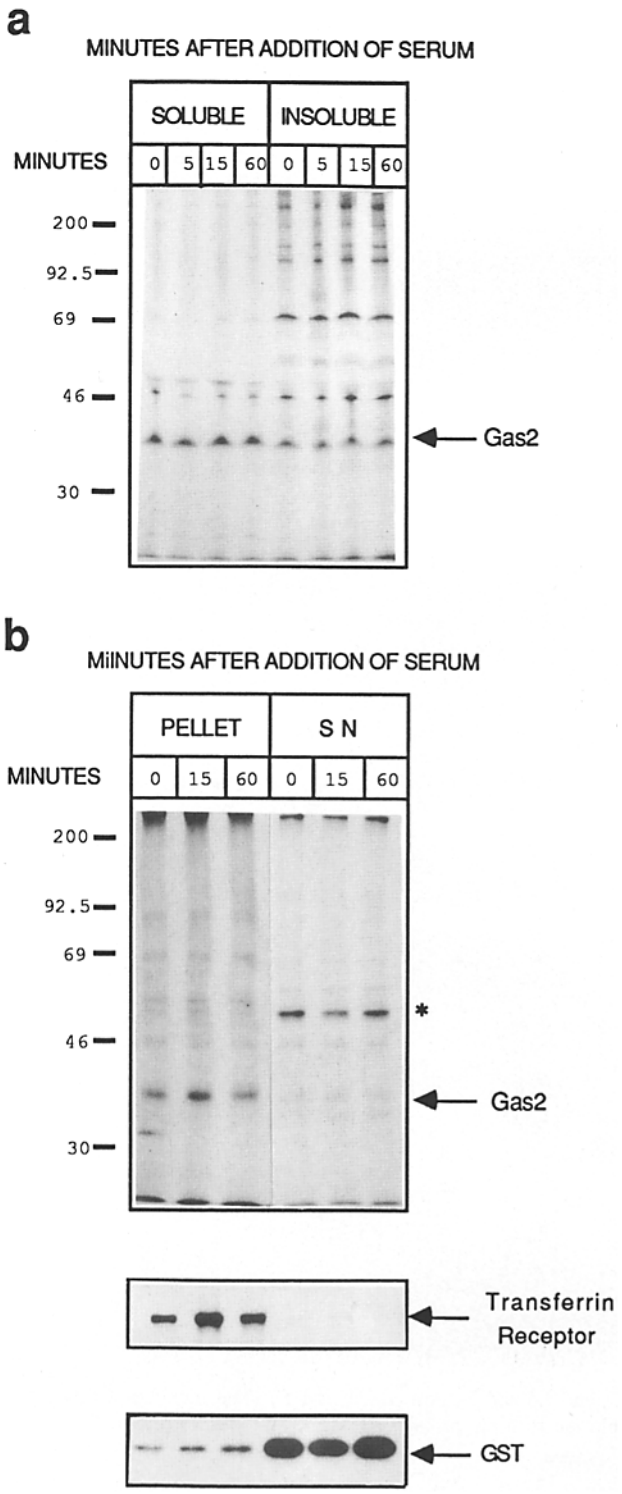

Figure 3. Distribution of ^{35}S-labeled Gas2 among subcellular fractions. (*a*) Detergent-soluble and -insoluble fractions from serum-starved NIH 3T3 (*0*) or serum activated for the indicated times were subjected to Gas2 immunoprecipitation. (*b*) immunoprecipitations analysis of Gas2 from crude membrane fraction (*PELLET*) or cytosolic fraction (*SN*) were performed on NIH 3T3 cells serum starved (*0*) or serum activated for the indicated times.

fiber formation. As shown in Fig. 4 (*D, arrow*) membrane ruffling is first noticed after 5 min from serum addition. At later times an increase in stress fibers (Fig. 4 *F*) across the whole length of the cell is observed.

The distribution of Gas2 in growth-arrested NIH 3T3 cells is predominantly concentrated as a mostly uniform layer along the edge of the cell and, albeit at lower intensity, along the stress fibers (see Fig. 4 *A*).

A change in Gas2 distribution is evident after 5 min. The clearest difference in Gas2 distribution is noticeable at the level of cell surface where bright structures; identified as membrane ruffling, are present (Fig. 4, *C* and *D, arrows*).

Although detectable already at early times rearrangements of the Gas2 distribution at the cellular edge are most dramatically evident when the analysis is performed after 1 h from serum stimulation (Fig. 4, *E* and *F, arrowhead*). At this time in fact the cell border, as decorated for Gas2 (Fig. 4 *E*), assumes a jigsaw profile which resembles the retraction fibers previously described in other cellular systems (9, 42). The Gas2 staining at the cellular edge appears to be concentrated in the area of cell–matrix interactions. This was confirmed by performing double-immunofluorescence analysis for Gas2 and talin (15), a well-known component of the adhesion plaques (data not shown). This analysis thus shows that exposure of quiescent cells to FCS results in a time dependent alteration of Gas2 distribution that is coupled to cell shape reorganization.

To clearly establish the redistribution of Gas2 in the ruffling membrane after serum stimulation we performed a laser scan microscopic analysis. The distribution of Gas2 and actin filaments, Gas2 and the cell surface protein: transferrin receptor, was compared in serum-starved and -stimulated cells. To illustrate the spatial relationship between the two different labels in the same specimen (Gas2 and actin or Gas2 and transferrin receptor) a series of optical sections was collected for each label in 0.3-μm steps.

As shown in Fig. 5 (*A* and *C*) Gas2 staining is concentrated at the cell border in quiescent cells (*yellow* or *green*), but after serum stimulation it redistributes to the newly formed membrane ruffling (Fig. 5 *B* and *D, arrows*) where it colocalizes with the actin filaments (Fig. 5 *B, yellow*). On the contrary, the transferrin receptor (*red dots*) is uniformly excluded from the cell border in quiescent cells (Fig. 5 *C*) and does not become concentrated in the membrane ruffles (Fig. 5 *D, arrows*) after serum stimulation. From this analysis we can conclude that Gas2 protein is specifically localized in the membrane ruffling during the first minutes of the Go→G1 transition in NIH 3T3 cells.

Analysis of Gas2 Phosphorylation, Expression, and Subcellular Localization after PDGF Treatment of Serum-starved Cells

Addition of growth factors to quiescent cells selectively induces the formation of membrane ruffling (6, 39). The most dramatic effect has been described when quiescent human foreskin fibroblasts are treated with PDGF (36, 37). The resulting unique membrane ruffling, formed by circular rearrangements at the dorsal side of the cells (circular membrane ruffling [CMR]) (36), has been proposed as a bioassay for PDGF (37). We thus analyzed the effects on the regulation of Gas2 phosphorylation, biosynthesis and cellular distribu-

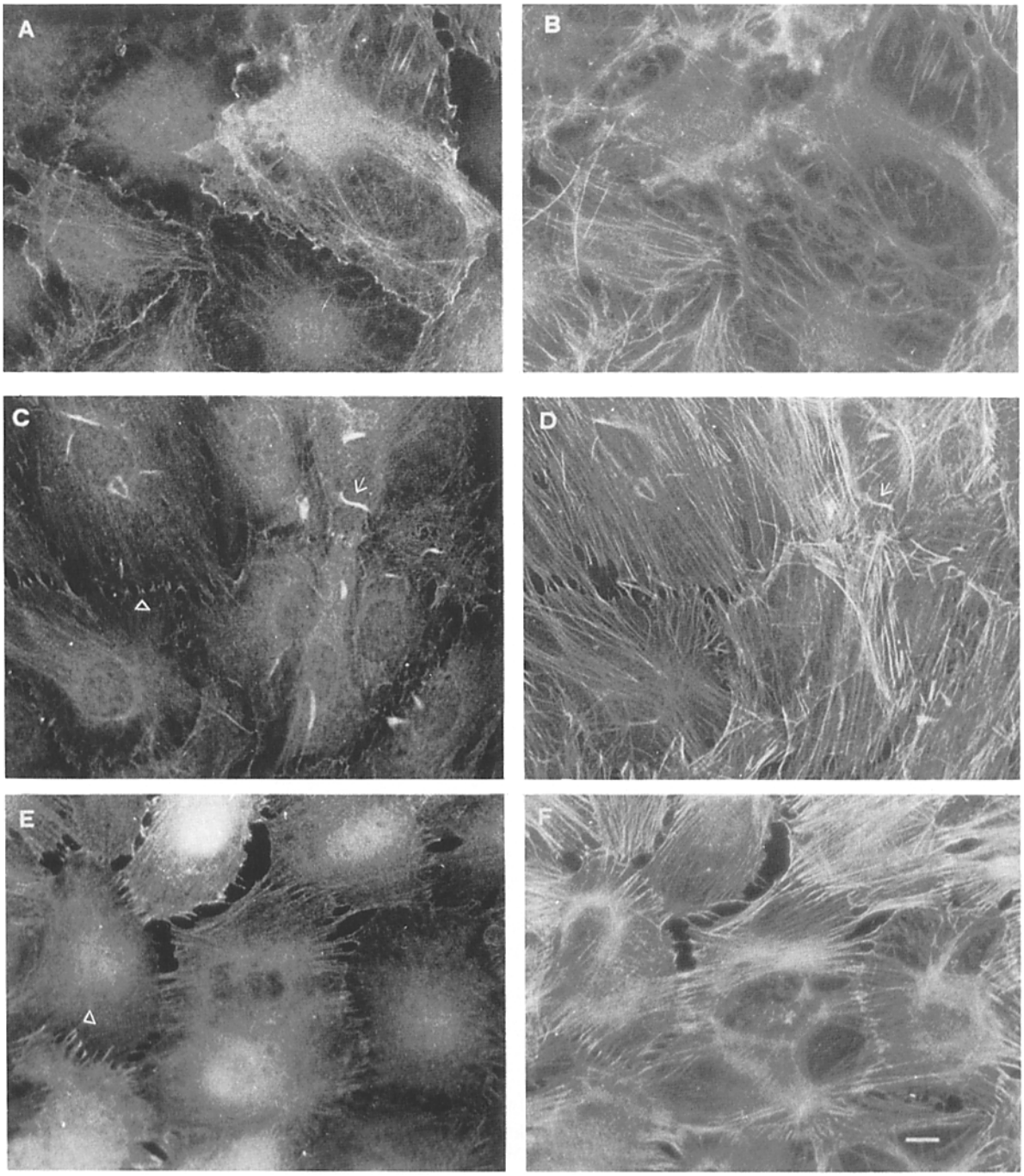

Figure 4. Effect of 20% FCS addition on the distribution of Gas2 (*A*, *C*, and *E*) and F-actin (*B*, *D*, and *F*). The incubation times were 0 min (*A* and *B*) 5 min (*C* and *D*) 1 h (*E* and *F*). Arrows indicate membrane ruffling, arrowheads indicate retraction fiber. Bar, 5 μm.

tion after treatment of serum-starved NIH 3T3 cells with PDGF.

The kinetics of in vivo Gas2 phosphorylation as elicited by PDGF is shown in Fig. 6 (*a*). It can be appreciated that, similarly to FCS, PDGF is able to induce the highest level of Gas2 phosphorylation as soon as 5-min poststimulation. This higher phosphorylation level is maintained until 30 min.

The response to PDGF was then analyzed for the down-regulation of Gas2 biosynthesis. The level of Gas2 biosynthesis is decreased with a similar kinetics as already observed when using FCS (5). In fact when cells were pulsed with [^{35}S]methionine during the first 3 h after PDGF addition a clear decrease in Gas2 biosynthesis is detectable (Fig. 6, *b*).

As a final step in this analysis we assayed the mitogenic effect of PDGF on the NIH 3T3 cellular system used: up to 70% of NIH 3T3 cells reach the S phase after 15 h from addi-

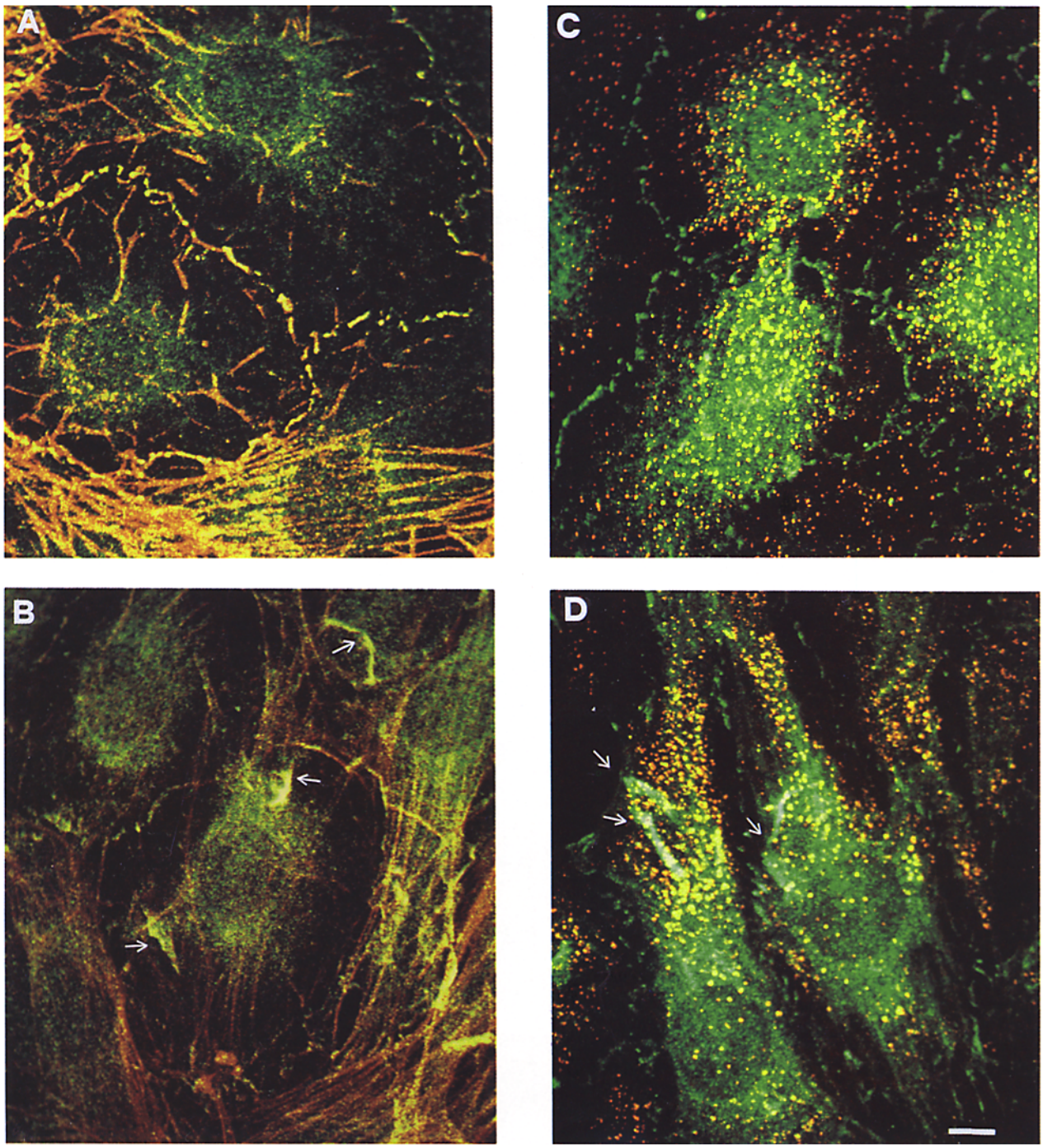

Figure 5. A confocal generated overlay showing the distribution of Gas2 (*green*) and actin (*red*) (*A* and *B*) or Gas2 (*green*) and transferrin receptor (*red*) (*C* and *D*) in serum-starved (*A* and *C*) or -stimulated (*B* and *D*) (5 min) NIH 3T3 cells. Immunofluorescence analysis was performed as described in material and methods. Images were overlayed using a Zeiss confocal microscope and are displayed in pseudocolor. Bar, 3 μm.

tion of 40 ng/ml of PDGF (Fig. 6 *c*). No increase in the percentage of cells in S phase was observed using PDGF at higher concentration (100 ng/ml).

Next we examined the subcellular distribution of Gas2 and actin by immunofluorescence analysis; the typical CMR as induced by PDGF in human foreskin fibroblast (37), are also present in NIH 3T3 cells.

Fig. 7 shows that multiple CMR, as detected by actin staining on the dorsal cellular surface, are present as soon as 5 min from PDGF addition (*D*) to serum-starved NIH 3T3 cells (*B*).

Gas2 distribution changes its typical pattern as observed in serum starved cells (Fig. 7 *A*) and clearly follows CMR formation where it becomes concentrated (*C* and *D*).

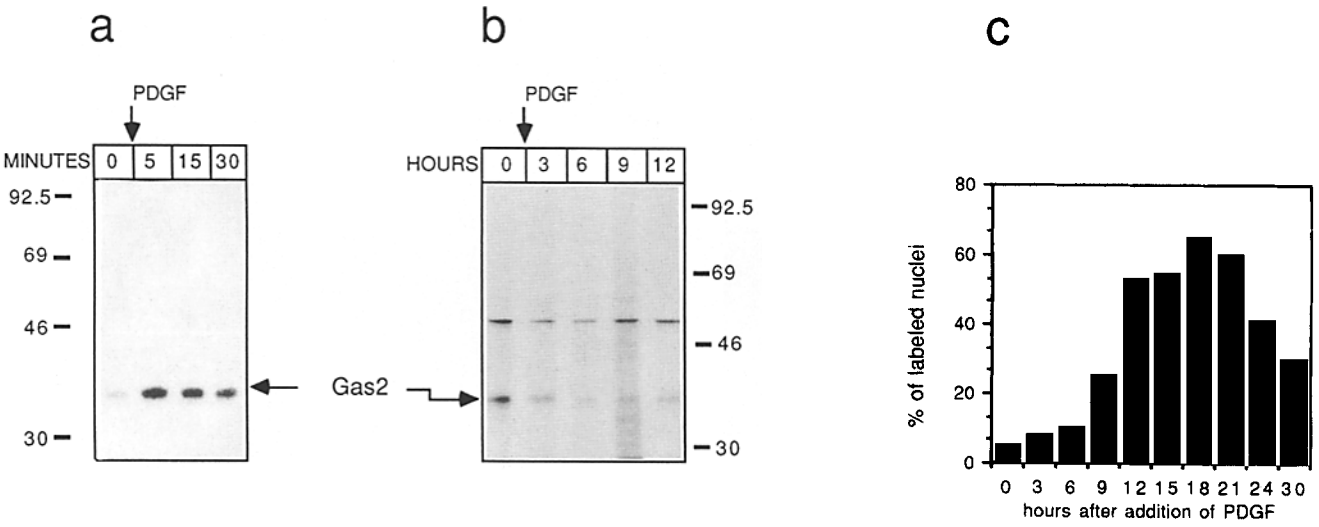

Figure 6. Analysis of Gas2 phosphorylation and expression after PDGF addition to serum starved NIH 3T3 cells. (*a*) Phosphorylation of Gas2 after addition of PDGF to serum-starved NIH 3T3 cells. Serum-starved NIH 3T3 cells (0) or after PDGF addition for the indicated times were prelabeled for 5 h with ^{32}Pi. After cell lysis, immunoprecipitations were performed using the same number of cpm. (*b*) Serum-starved NIH 3T3 cells were treated with PDGF for the indicated times and labeled with [^{35}S]methionine for 3 h before cell lysis. Immunoprecipitations were performed using the same number of cpm. (*c*) BrdUrd incorporation is shown in diagram analysis.

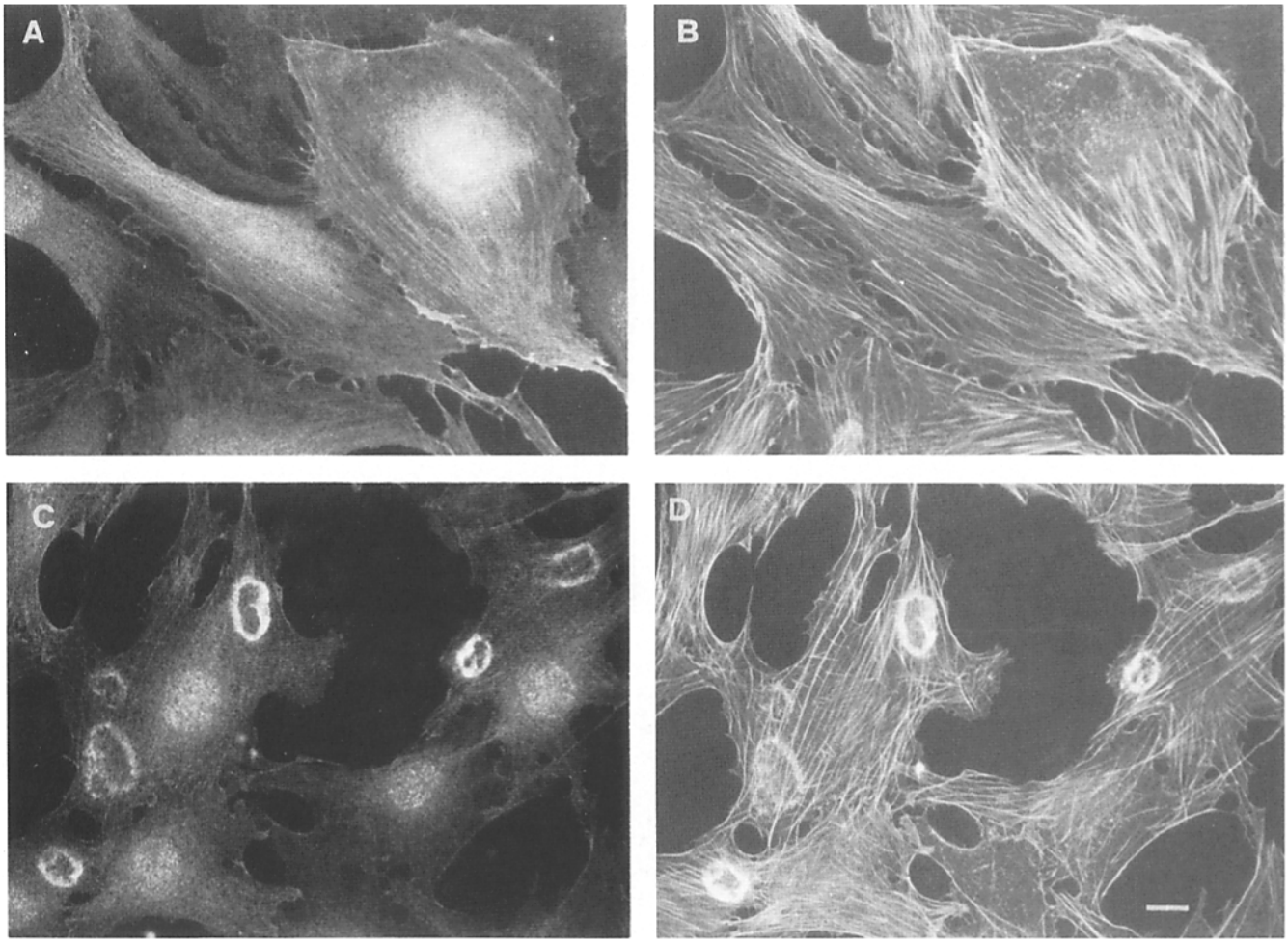

Figure 7. Effect of PDGF addition to serum starved NIH 3T3 cells on the distribution of Gas2 (*A* and *B*) and F-actin (*C* and *D*). The incubation times were 0 min (*A* and *B*) and 5 min (*C* and *D*). Bar, 5 μm.

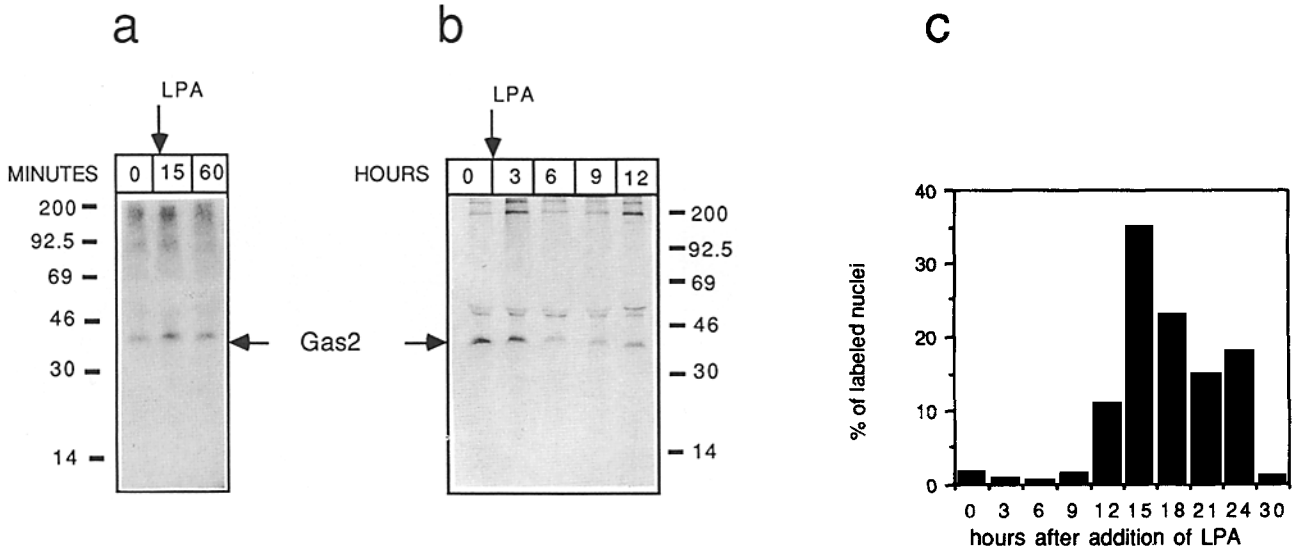

Figure 8. Analysis of Gas2 phosphorylation and expression after LPA addition to serum starved NIH 3T3 cells. (*a*) Phosphorylation of Gas2 after addition of LPA to serum-starved NIH 3T3 cells. Serum-starved NIH 3T3 (*0*) or after LPA addition for the indicated times were prelabeled for 5 h with ^{32}Pi. After cell lysis, immunoprecipitations were performed using the same number of cpm. (*b*) Serum-starved NIH 3T3 cells were treated with PDGF for the indicated times and labeled with [^{35}S]methionine for 3 h before cell lysis. Immunoprecipitations were performed using the same number of cpm. (*c*) BrdUrd incorporation is shown in diagram analysis.

Analysis of Gas2 Phosphorylation, Expression, and Subcellular Localization after LPA Treatment of Serum-starved Cells

A modification of the actin architecture as elicited by serum during the Go→G1 transition in NIH 3T3 cells is an increased length and number of stress fibers. It has recently been demonstrated that an effector of this cellular response is the serum component lysophosphatidic acid (LPA) (38).

We thus analyzed the ability of LPA to induce Gas2 hyperphosphorylation. LPA was used at a concentration of 70 μM, displaying the highest mitogenic activity on REF52 cells and human fibroblasts (55).

As shown in Fig. 8 *a*, LPA fails to determine a clear increase of Gas2 phosphorylation both at short (15 min) or long times (60 min) after stimulation. On the contrary LPA is able to down-regulate Gas2 biosynthesis albeit with a slower kinetic when compared to 20% FCS or PDGF. In fact during the first 3 h after LPA addition to serum-starved NIH 3T3 cells, there is no appreciable downregulation of Gas2 biosynthesis, which becomes evident only in the following 3 h (Fig. 8 *b*).

We next analyzed the mitogenic effect of LPA on NIH 3T3 cells cultured for 48 h in 0.5% FCS. LPA is a weak mitogen when compared to PDGF or 20% FCS. In fact a maximum of 35% of the cells appear to enter in S phase after 15 h from LPA stimulation (Fig. 8 *c*).

It has been demonstrated that addition of LPA to Swiss 3T3 cells cultured in the absence of serum rapidly induces formation of stress fibers and focal adhesions (38). Fig. 9 shows the immunofluorescence analysis for Gas2 and actin distribution in NIH 3T3 cells after various times from LPA addition. Fig. 9 (*A* and *B*) show the usual pattern of Gas2 and actin, respectively, in serum-starved NIH 3T3 cells. After 15 min from LPA addition changes in actin distribution are evident: stress fibers now are organized throughout the length of the cells and their number is apparently increased. Gas2 distribution follows the modifications at the cell border already described for 20% FCS, where the cellular edge becomes indented (see Fig. 4). These changes in actin architecture are even more evident when the analysis is performed after 60 min from LPA stimulation (Fig. 9, *E* and *F*). We can thus conclude that Gas2 phosphorylation is uncoupled from the reorganization of stress fibers as induced by LPA.

Analysis of Gas2 Phosphorylation, Expression, and Subcellular Localization after PMA Treatment of Serum-starved Cells

To further strengthen the correlation between changes in Gas2 phosphorylation and membrane ruffling we decided to use mitogens that do not signal through tyrosine kinase receptor. We chose PMA since it is well known to induce a wide range of responses, such as changes in shape, stimulation of DNA synthesis, and cell growth (33, 40, 57).

A clone of NIH 3T3 cells (NIH 3T3/A) with a high mitogenic response to PMA was used for this study. Similarly to what has been shown for the other mitogens, we first analyzed if Gas2 hyperphosphorylation is induced in NIH 3T3/A in response to PMA. Fig. 10 *a* shows the kinetics of in vivo Gas2 phosphorylation as elicited by PMA. Unlike FCS and PDGF, it is apparent that the kinetics of phosphorylation induced by PMA is delayed. Hyperphosphorylation becomes evident only after 15 min and steadily increases to reach a maximum level at 30 min from PMA addition.

We next analyzed the effect of PMA on the level of Gas2 biosynthesis. Fig. 10 (panel *b*) shows the immunoprecipitation analysis of Gas2 from a 3 h [^{35}S]methionine labeling of quiescent cells and after different times from PMA addition. At difference with 20% FCS and PDGF, the level of Gas2

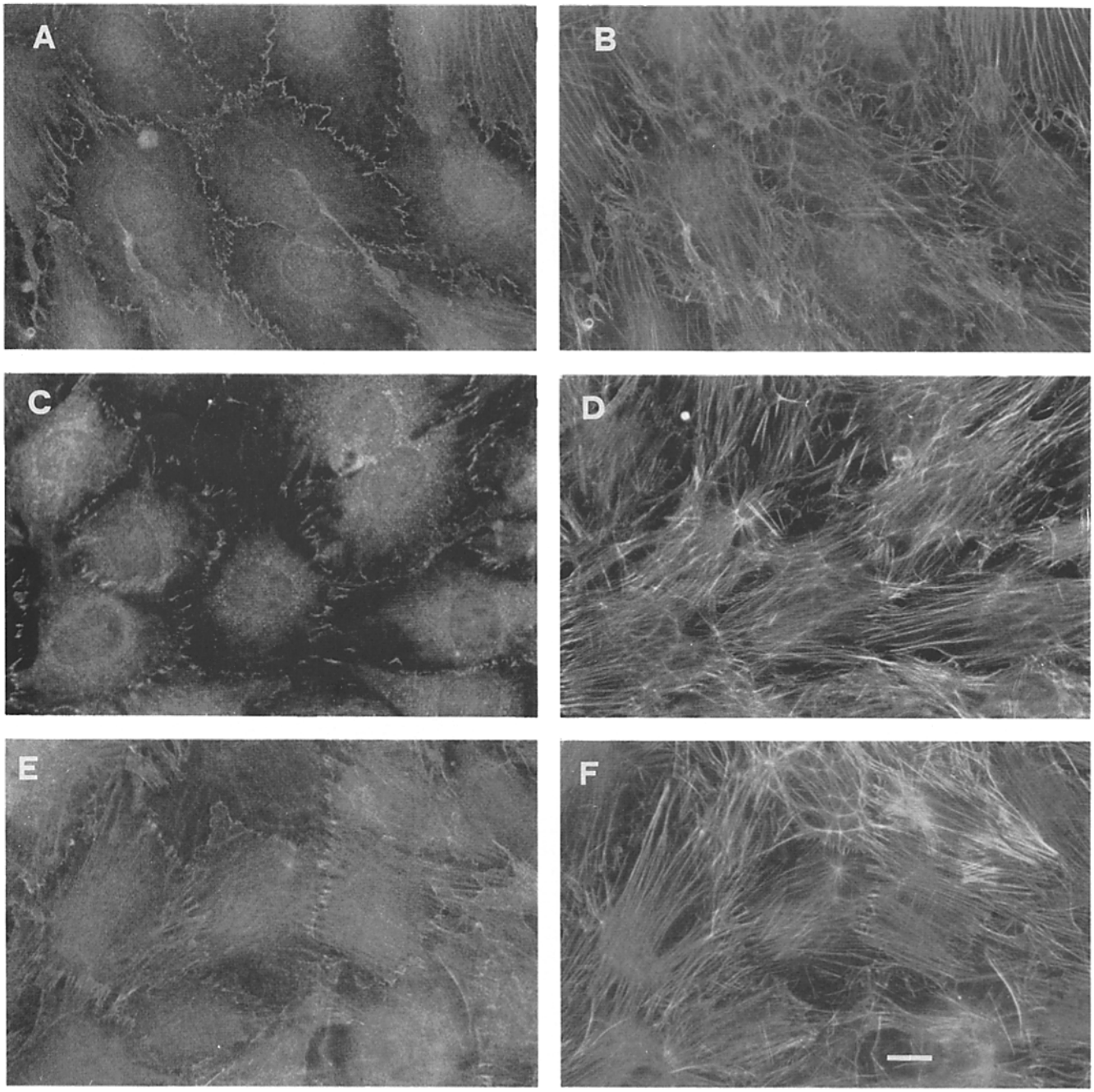

Figure 9. Effect of LPA addition to serum-starved NIH 3T3 cells on the distribution of Gas2 (*A*, *C*, and *E*) and F-actin (*B*, *D*, and *F*). The incubation times were 0 min (*A* and *B*), 15 min (*C* and *D*), and 60 min (*E* and *F*). Bar, 5 μm.

biosynthesis does not appreciably drop within the first 3 h from PMA addition. However in the following 3 h its level is markedly reduced and remains lower for the following times, with a behavior similar to that observed after addition of LPA to quiescent cells.

Fig. 10 (*c*) shows the analysis of DNA synthesis as revealed by BrdUrd incorporation after treatment of serum-starved cells with 10^{-7} M PMA. The highest number of cells in S phase (67%) is detected after 15 h from PMA addition. Thus, PMA treatment of serum-starved NIH 3T3/A cells elicits cellular responses that include both down-regulation of Gas2 biosynthesis and an increased level of Gas2 phosphorylation as already described for serum (5), both responses showing an apparently slower kinetics.

A number of studies with different cellular systems has firmly established that treatment of cells with phorbol esters induces dramatic and rapid changes of their morphology and in particular of the actin cytoskeleton (40, 43, 48). The most pronounced effect is a dose- and time-dependent dissolution of the stress fibers that accompanies the formation of extended membrane ruffles (43).

Fig. 11 shows the kinetics of alterations that were observed

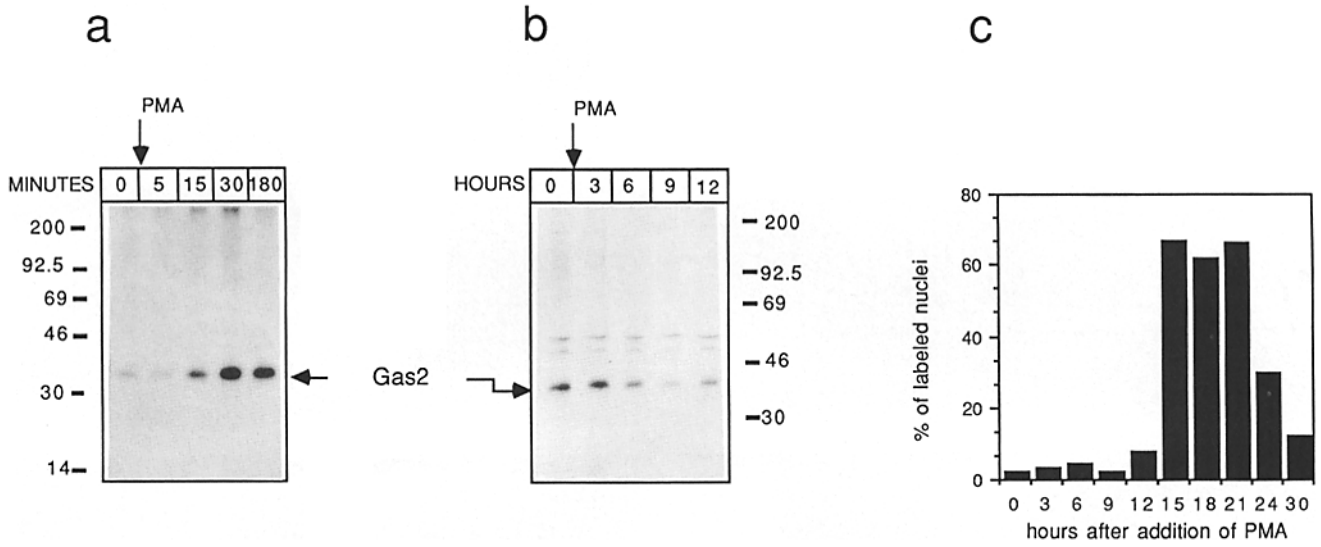

Figure 10. Analysis of Gas2 phosphorylation and expression after PMA addition to serum starved NIH 3T3/A cells. (*a*) Phosphorylation of Gas2 after addition of PMA to serum-starved NIH 3T3 cells. Serum-starved NIH 3T3 (*0*) or after PMA addition for the indicated times were prelabeled for 5 h with ^{32}Pi. After cell lysis, immunoprecipitations were performed using the same number of cpm. (*b*) Serum-starved NIH 3T3 cells were treated with PMA for the indicated times and labeled with [^{35}S]methionine for 3 h before cell lysis. Immunoprecipitations were performed using the same number of cpm. (*c*) BrdUrd incorporation is shown in diagram analysis.

in NIH 3T3/A cells after treatment with PMA. Both in serum-starved NIH 3T3/A cells (Fig. 11, *A* and *B*) or after 5 min from PMA addition (Fig. 11, *C* and *D*) a similar distribution of Gas2 (*A* and *C*) and actin filaments (*C* and *D*) is observed that is typically found in growth arrested cells. Only after 15 min from PMA addition an increased number of membrane ruffles at the cell periphery is clearly detected (Fig. 11, *E* and *F*). This phenomenon thus seems to coincide with the increased level of Gas2 phosphorylation (see Fig. 10 *a*) which, at difference with FCS and PDGF, starts at 15 min and steadily increases up to 30 min from PMA addition.

A parallel increase in the number of cells showing rearrangements in their morphology and in the intensity of such alterations is detected (Fig. 11, *G* and *H*) after 30 min, when the stress fibers are no longer visible.

Thus PMA induces dramatic changes in both actin filament organization and Gas2 distribution and the timing of these changes correlates with the kinetics of Gas2 phosphorylation as induced by PMA.

Discussion

There is a growing interest in understanding the molecular processes that underlie growth arrest. We have approached this problem by cloning and characterizing genes that are specifically expressed during growth arrest (4, 5, 14, 34, 35, 45).

In a previous work we have shown that *gas2* is an evolutionary conserved component of the microfilament system. The level of Gas2 protein steadily increases when cell growth is restricted but, due to its long half-life, it does not become appreciably down-regulated during Go→G1 transition.

In this work we extend a preliminary observation that established an increased level of Gas2 phosphorylation during Go→G1 transition. We show here that Gas2 is hyperphosphorylated in serine residues within 5 min from serum stimulation of growth-arrested NIH 3T3 cells, and this level of phosphorylation is maintained for at least 3 h after stimulation. Using an in vitro assay we have been able to dissect the timing of activation of the Gas2-specific kinase(s). Its full activity is reached after 10 min from serum addition and is maintained for the next 3 h. Since Gas2 is a component of the microfilament system we have analyzed its subcellular distribution during Go→G1 transition as induced by serum. By immunofluorescence analysis a most clear redistribution of Gas2 becomes apparent at the level of membrane ruffling on the dorsal side of the cell within 5 min from serum addition, thus suggesting a correlation between Gas2 hyperphosphorylation and its subcellular redistribution. A concomitant reorganization of Gas2 distribution at the cellular edge into the newly formed retraction fibers (9, 42) is observed, which becomes more evident at later times.

Major alterations of the microfilament system occurring during the Go→G1 transition have been identified, namely: (*a*) induction of membrane ruffling; and (*b*) formation of stress fiber (38, 39). These two changes have been recently dissected through their association with different extracellular stimuli and thus transduction pathways. LPA has been shown to be responsible for stress fibers and adhesion plaque formation (38) while PDGF and other growth factors are mainly responsible for membrane ruffling (39). In this context the different signal transducing mechanisms have been demonstrated to be dependent on small GTP-binding proteins of the *ras* family *rho* (stress fibers) and *rac* (membrane ruffling) (38, 39).

By the use of PDGF and LPA we have analyzed whether Gas2 hyperphosphorylation is coupled to membrane ruffling or stress fiber formation. PDGF is a potent inducer of Gas2 hyperphosphorylation which correlates temporally with the appearance of the typical CMR (36), where Gas2 becomes

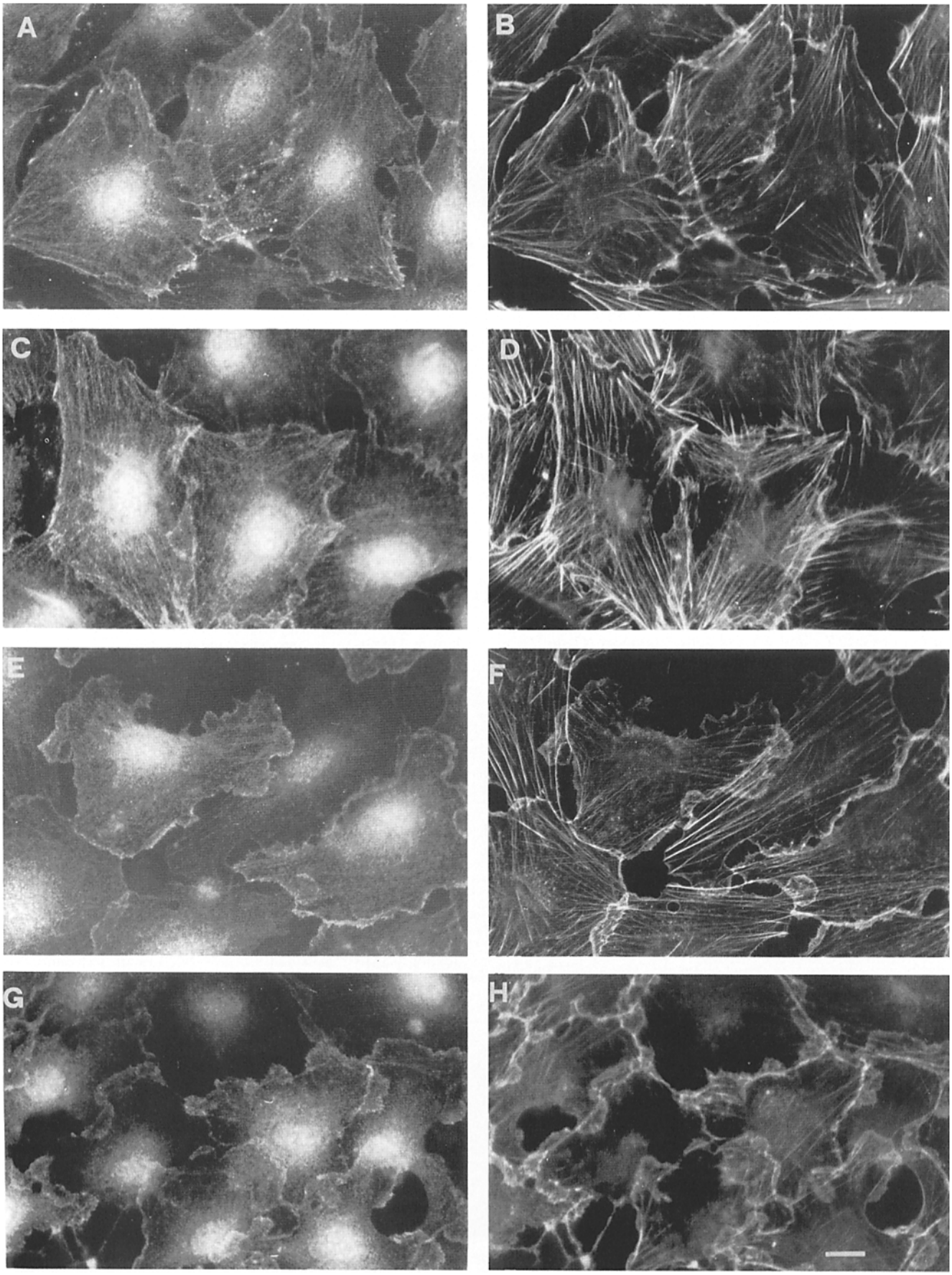

Figure 11. Effect of PMA addition to serum starved NIH 3T3/A cells on the distribution of Gas2 (*A*, *C*, *E*, and *G*) and F-actin (*B*, *D*, *F*, and *H*). The incubation times were 0 min (*A* and *B*), 5 min (*C* and *D*), 15 min (*E* and *F*), and 30 min (*G* and *H*). Bar, 5 μm.

localized. LPA, on the other hand, has the ability to induce stress fiber formation, but fails to induce an appreciable Gas2 hyperphosphorylation. Thus Gas 2 hyperphosphorylation correlates with membrane ruffling formation and does not seem to be related to the formation of stress fibers as mediated by LPA.

Ruffling formation is caused by actin polymerization at the inner surface of the plasma membrane and occurs predominantly during cell spreading and locomotion in cultured cells (49). It has been demonstrated that a specific type of membrane ruffling, as induced by PDGF (CMR) is dependent on the activation of the β type, but not the α type, of PDGF receptor (17, 56). In this context it has been proposed that CMR formation is related to a chemotactic and motility response which is triggered by activation of the β-PDGF but not of the α-PDGF receptor (17, 56). Another well-known inducer of membrane ruffling is PMA (39): in this case membrane-ruffing formation is most prominent at the cellular edge and is accompanied by the disappearance of stress fibers and a concomitant drastic morphological change (40, 43, 48).

Also in this case we have demonstrated a tight correlation between Gas2 hyperphosphorylation and the appearance of membrane ruffling at the cellular edge, where Gas2 is localized. The kinetics of these phenomena are obviously delayed with respect to PDGF due to involvement of different classes of kinases, tyrosine receptor kinase in the case of PDGF and PKC in the case of PMA (29).

An important target for PKC, MARCKS the myristoylated alanine-rich C kinase substrata (MARCKS) (20) is an actin cross-linking protein whose activity is inhibited by PKC-mediated phosphorylation and by the binding to calcium/calmodulin (23). In this context it is interesting to note that expression of MARCKS is highly induced in growth arrested fibroblasts and becomes down-regulated during Go→G1 transition (25). However, MARCKS phosphorylation by PKC is strictly related to a shift in its distribution from a membrane to a cytosolic compartment (50), whereas this does not seem to hold true for Gas2. By biochemical fractionation we have demonstrated that Gas2 is mainly membrane associated and this distribution does not appear to change during Go→G1 transition. Moreover, by mild detergent extraction we have shown that Gas2 is equally partitioned in the detergent-soluble and -insoluble fractions and that this ratio is not changed during Go→G1 transition.

We would thus argue that Gas2 hyperphosphorylation is not responsible for mediating changes between different subcellular compartments, although we cannot exclude a role in inducing finer changes within specific cellular districts such as the cellular cortex. We favor the hypothesis that Gas2 hyperphosphorylation could be a mean to interfere with its function, which is presumably related to its growth arrest-specific expression. In fact cellular responses dependent on the microfilament system (e.g., cell motility) are dramatically restricted in quiescent cells (10). This could imply the existence of specific elements required for the organization of such cytoskeletal related restrictions: Gas2 could thus represent one of these elements and its phosphorylation could relieve this function.

Recently a candidate tumor suppressor gene for the type 2 neurofibromatosis (merlin-schwannomin) has been shown to present a striking homology to a family of proteins proposed to link the cytoskeleton to the plasma membrane (41, 52). This discovery implicates that tumor suppressor gene products are also localized at the level of the cytoskeletal plasma membrane interaction sites, thus opening the possibility that Gas2 function may also lie within this context.

We would like to thank Mr. M. Benedetti for performing part of the immunofluorescence studies, Mr. Carlo Albride (Zeiss Italia) for help with confocal analysis and Dr. M. Zanetti for critically reading the manuscript.

This work was supported by Associazione Italiana Ricerca sul Cancro (AIRC) as part of the special project "Oncosuppressor genes". C. Brancolini is an AIRC fellow.

Received for publication 12 July 1993 and in revised form 21 October 1993.

References

1. Aaronson, S. A. 1991. Growth factors and cancer. *Science (Wash. DC).* 254:1146–1153.
2. Aderem, A. 1992. Signal transduction and the actin cytoskeleton: the roles of MARCKS and profilin. *Trends Biochem. Soc.* 17:438–443.
3. Bockus, B. J., and C. D. Stiles. 1984. Regulation of cytoskeletal architecture by platelet-derived growth factor, insulin and epidermal growth factor. *Exp. Cell. Res.* 153:186–197.
4. Brancolini, C., and C. Schneider. 1991. Change in the expression of a nuclear matrix-associated protein is correlated with cellular transformation. *Proc. Natl. Acad. Sci. USA.* 88:6936–6940.
5. Brancolini, C., S. Bottega, and C. Schneider. 1992. Gas2, a growth arrest-specific protein, is a component of the microfilament network system. *J. Cell Biol.* 117:1251–1261.
6. Bretscher, A. 1989. Rapid phosphorylation and reorganization of ezrin and spectrin accompany morphological changes induced in A-431 cells by epidermal growth factor. *J. Cell Biol.* 108:921–930.
7. Brooks, S. F., T. Herget, S. Broad, and E. Rozengurt. 1992. The expression of 80K/MARCKS, a major substrate of protein kinase c (PKC), is down-regulated through both PKC-dependent and -independent pathways. *J. Biol. Chem.* 267:14212–14218.
8. Chao, M. V. 1992. Growth factor signaling: where is the specificity? *Cell.* 68:995–997.
9. Chinkers, M., J. A. McKanna, and S. Choen. 1979. Rapid induction of morphological changes in human carcinoma cells A-431 by epidermal growth factor. *J. Cell Biol.* 83:260–265.
10. Conrad, P. A., K. A. Giuliano, G. Fisher, K. Collins, P. T. Matsudaira, and D. L. Taylor. 1993. Relative distribution of actin, myosin I, myosin II during the wound healing response to fibroblasts. *J. Cell Biol.* 120:1381–1391.
11. Coughlin, S. R., W. M. F. Lee, P. W. Williams, G. M. Giels, and L. T. Williams. 1985. c-myc gene expression is stimulated by agents that activate protein kinase C and does not account for mitogenic effect of PDGF. *Cell.* 43:243–251.
12. Courtneidge, S. A., A. D. Levinson, and J. M. Bishop. 1980. The protein encoded by the transforming gene of avian sarcoma virus ($pp60^{src}$) and a homologous protein in normal cells ($pp60^{proto\text{-}src}$) are associated with the plasma membrane. *Proc. Natl. Acad. Sci. USA.* 77:3783–3787.
13. Davis, S., M. L. Lu, S. H. Lo, S. Lin, J. A. Butler, B. J. Druker, T. M. Roberts, Q. An, and L. B. Chen. 1991. Presence of an SH2 domain in the actin-binding protein tension. *Science (Wash. DC).* 252:712–715.
14. Del Sal, G., M. E. Ruaro, L. Philipson, and C. Schneider. 1992. The growth arrest-specific gene gas1 is involved in growth suppression. *Cell.* 70:595–607.
15. DePasquale, J. A., and C. S. Izzard. 1991. Accumulation of talin in nodes at the edge of the lamellipodium and separate incorporation into adhesion plaque at focal contacts in fibroblasts. *J. Cell Biol.* 113:1351–1359.
16. Erikson, R. L. 1991. Structure, expression, and regulation of protein kinase involved in the phosphorylation of ribosomal protein S6. *J. Biol. Chem.* 266:6007–6010.
17. Eriksson, A., A. Seibahn, B. Westermark, C.-H. Heldin, and L. Claesson-Welsh. 1992. PDGF α- and β-receptors activate unique and common signal transduction pathways. *EMBO (Eur. Mol. Biol. Organ.) J.* 11: 543–550.
18. Gluck, U., J. I. Rodriguez-Fernandez, R. Pankov, and A. Ben Ze'ev. 1992. Regulation of adherens junction protein expression in growth activated 3T3 cells and regenerating liver. *Exp. Cell Res.* 202:477–486.
19. Goldschmidt-Clermont, P. J., and P. A. Janmey. 1991. Profilin a weak CAP for actin and RAS. *Cell.* 66:419–421.
20. Graff, J. M., J. I. Gordon, and P. J. Blackshear. 1989. Myristoylated and nonmyristoylated forms of a protein are phosphorylated by protein kinase C. *Science (Wash. DC).* 246:503–506.
21. Greenberg, M. E., and E. B. Ziff. 1984. Stimulation of 3T3 cells induces transcription of the c-fos proto-oncogene. *Nature (Lond.).* 311:433–438.

22. Hartwig, J. H. 1992. An ultrastructural approach to understanding the cytoskeleton. *In* The Cytoskeleton a Practical Approach. K. L. Carraway and C. A. C. Carraway, editors. IRL, Oxford University Press, New York. 23–45.
23. Hartwig, J. H., M. Thelen, A. Rosen, P. A. Janmey, A. C. Nairn, and A. Aderem. 1992. MARCKS is an actin filament crosslinking protein regulated by protein kinase C and calcium-calmodulin. *Nature (Lond.).* 356: 618–622.
24. Heikkila, R., G. Schwab, E. Wickstrom, S. Loong Loke, D. H. Pluznik, R. Watt, and L. M. Neckers. 1987. A c-myc antisense oligideoxynucleotide inhibits entry into S phase but not progress from Go to G1. *Nature (Lond.).* 328:445–449.
25. Herget, T., S. F. Brooks, S. Broad, and E. Rozengurt. 1993. Expression of the major protein kinase C substrate, the acidic 80-kilodalton myristoylated alanine-rich C kinase substrate, increases sharply when Swiss 3T3 cells move out of cycle. *Proc. Natl. Acad. Sci. USA.* 90:2945–2949.
26. Herman, B., and W. J. Pedger. 1985. Platelet-derived Growth factor-induces alterations in vinculin and actin distribution in BALB/c-3T3 cells. *J. Cell Biol.* 100:1031–1040.
27. Herschman, H. R. 1991. Primary response genes induced by growth factors and tumor promoter. *Annu. Rev. Biochem.* 60:281–319.
28. Kamps, M. P. 1991. Determination of phosphoamino acid composition by acidic hydrolysis of protein blotted to immobilon. *In* Methods in Enzymology. T. Hunter, and B. M. Sefton, editors. Academic Press, Inc., New York. 201:21–27.
29. Kikkawa, U., A. Kishimoto, and Y. Nishizuka. 1989. The protein kinase C family: heterogeneity and its implications. *Annu. Rev. Biochem.* 58: 31–44.
30. Koch, C. A., D. Anderson, M. F. Moran, C. Ellis, and T. Pawson. 1991. SH2 and SH3 domains: elements that control interactions of cytoplasmic signaling proteins. *Science (Wash. DC).* 252:668–674.
31. Kovary, K., and R. Bravo. 1991. The Jun and Fos protein families are both required for cell cycle progression in fibroblasts. *Mol. Cell. Biol.* 11:4466–4472.
32. Kyriakis, J. M., H. App, X.-f. Zhang, P. Banerjee, D. L. Brautigan, U. R. Rapp, and J. Avruch. 1992. Raf-1 kinase activates MAP Kinase-kinase. *Nature (Lond.).* 358:417–421.
33. Laszlo, A., K. Radke, S. Chin, and M. J. Bissel. 1981. Tumor promoters alter gene expression and protein phosphorylation in avian cells in culture. *Proc. Natl. Acad. Sci. USA.* 78:6241–6245.
34. Manfioletti, G., E. Ruaro, G. Del Sal, L. Philipson, and C. Schneider. 1989. A growth arrest-specific (*gas*) gene codes for a membrane protein. *Mol. Cell. Biol.* 10:2924–2930.
35. Manfioletti, G., C. Brancolini, G. Avanzi, and C. Schneider. 1993. A growth arrest-specific gene (*gas6*) is a new member of the vitamin K-dependent proteins related to protein S, a negative coregulator in the blood coagulation. *Mol. Cell. Biol.* 13:4976–4985.
36. Mellestrom, K., A.-S. Höglund, M. Nister, C.-H. Heldin, B. Westermark, and U. Linberg. 1983. The effect of platelet-derived growth factor on morphology and motility of human glial cells. *J. Muscle Res. Cell Motil.* 4:589–609.
37. Mellstrom, K., C.-H. Heldin, and B. Westermark. 1988. Induction of circular membrane ruffling on human fibroblasts by platelet-derived growth factor. *Exp. Cell. Res.* 177:347–359.
38. Ridley, A. J., and A. Hall. 1992. The small GTP-binding protein rho regulates the assembly of focal adhesions and actin stress fibers in response to growth factors. *Cell.* 70:389–399.
39. Ridley, A. J., H. F. Paterson, C. L. Johnston, D. Diekmann, and A. Hall. 1992. The small GTP-binding protein rac regulates growth factor-induced membrane ruffling. *Cell.* 70:401–410.
40. Rifkin, D. B., R. M. Crowe, and R. Pollack. 1979. Tumor promoters induce changes in the chick embryo fibroblast cytoskeleton. *Cell.* 18: 361–368.
41. Rouleau, G. A., P. Merel, M. Lutchman, M. Sanson, J. Zucman, C. Marineau, K. Hoang-Xuan, S. Demczuk, C. Desemaze, B. Pluogastel, S. M. Pulst, G. Lenoir, E. Bijlsma, R. Fashold, J. Dumanski, P. de Jong, D. Parry, R. Eldrige, A. Aurias, O. Delattre, and G. Thomas. 1993. Alteration in a new gene encoding a putative membrane-organizing protein causes neuro-fibromatosis type 2. *Nature (Lond.).* 363:515–521.
42. Schlessinger, J., and B. Geiger. 1981. Epidermal growth factor induces redistribution of actin and α-actinin in human epidermal carcinoma cells. *Exp. Cell. Res.* 134:273–279.
43. Schliwa, M., T. Nakamura, K. R. Porter, and U. Eutener. 1984. A tumor promoter induces rapid and coordinated reorganization of actin and vinculin in cultured cells. *J. Cell Biol.* 99:1045–1059.
44. Schneider, C., R. Sutherland, R. Newman, and M. Greaves. 1982. The structural features of the cell surfaces receptor for transferrin that is recognized by the monoclonal antibody OKT9. *J. Biol. Chem.* 257:8516–8522.
45. Schneider, C., R. M. King, and L. Philipson. 1988. Genes specifically expressed at growth arrest of mammalian cells. *Cell.* 54:787–793.
46. Schneider, C., G. Del Sal, C. Brancolini, S. Gustincich, G. Manfioletti, and M. E. Ruaro. 1992. The growing biological scenario of growth arrest. *In* DNA Replication and Cell Cycle. E. Fanning, R. Knippers, and E.-L. Winnacker, editors, Springer-Verlag, Berlin/Heidelberg. 259–266.
47. Smith, D. B., and K. S. Johnson. 1988. Single-step purification of polypeptides expressed in *Escherichia coli* as fusions with glutathione S-transferase. *Gene.* 67:31–40.
48. Soube, K., Y. Fujio, and K. Kanda. 1988. Tumor promoter induces reorganization of actin filaments and calspectin (fodrin or non-erythroid spectrin) in 3T3 cells. *Proc. Natl. Acad. Sci. USA.* 85:482–486.
49. Stossel, T. P. 1993. On the crawling of animal cells. *Science (Wash. DC).* 260:1086–1094.
50. Thelen, M., A. Rosen, A. C. Nairn, and A. Aderem. 1991. Regulation by phosphorylation of reversible association of a myristoylated protein kinase C substrate with the plasma membrane. *Nature (Lond.).* 351:320–322.
51. Thomas, G. 1992. MAP kinase by any other name smells just as sweet. *Cell.* 68:3–6.
52. Trofatter, J. A., M. M. MacCollin, J. L. Rutter, J. R. Murrel, M. P. Duayo, D. M. Parry, R. Eldridge, N. Kley, A. G. Menon, K. Pulaski, V. H. Haase, C. M. Ambrose, D. Munroe, C. Bove, J. L. Haines, R. L. Martuza, M. E. MacDonald, B. R. Seizinger, M. P. Short, A. J. Buckler, and J. F. Gusella. 1993. A novel moesin-, ezrin-, radixin-like gene is a candidate for the neurofibromatosis 2 tumor suppressor. *Cell.* 72:791–800.
53. Ullrich, A., and J. Schlessinger. 1990. Signal transduction by receptor with tyrosine kinase activity. *Cell.* 61:203–212.
54. Ungar, F., B. Geiger, and A. Ben-Ze'ev. 1986. Cell contact- and shape-dependent regulation of vinculin synthesis in cultured fibroblasts. *Nature (Lond.).* 319:787–791.
55. van Corven, E. J., A. Groenink, K. Jalink, T. Eichholtz, and W. H. Moolenaar. 1989. Lysophosphatidate-induced cell proliferation: identification and dissection of signaling pathways mediated by G proteins. *Cell.* 59:45–54.
56. Westermark, B., A. Siegbhan, C.-H. Heldin, and L. Claesson-Welsh. 1990. β-type receptor for platelet-derived growth factor mediates a chemotactic response by means of ligand-induced activation of the receptor protein-tyrosine kinase. *Proc. Natl. Acad. Sci. USA.* 87:128–132.
57. Yuspa, S. H., U. Lichti, T. Ben, E. Patterson, H. Hennings, T. Slaga, N. Colburn, and W. Klesey. 1976. Phorbol esters stimulate DNA synthesis and ornithine decarboxylase activity in mouse epidermal cultures. *Nature (Lond.).* 263:402–404.